2012

Nonexponential Solid State 1H and 19F Spin−Lattice Relaxation, Single-crystal X-ray Diffraction, and Isolated-Molecule and Cluster Electronic Structure Calculations in an Organic Solid: Coupled Methyl Group Rotation and Methoxy Group Libration in 4,4'-Dimethoxyoctafluorobiphenyl

Donald P. Fahey

William G. Dougherty Jr

W. Scott Kassel

Xianlong Wang

Peter A. Beckmann
Bryn Mawr College, pbeckman@brynmawr.edu

Nonexponential Solid State ^{1}H and ^{19}F Spin-lattice Relaxation, Single-crystal X-ray Diffraction, and Isolated-molecule and Cluster Electronic Structure Calculations in an Organic Solid: Coupled Methyl Group Rotation and Methoxy Group Libration in 4,4'-Dimethoxyoctafluorobiphenyl

Donald P. Fahey,[†] William G. Dougherty Jr.,[×] W. Scott Kassel,[×] Xianlong Wang,[§, *] and Peter A. Beckmann,[†, *]

Department of Physics, Bryn Mawr College, 101 North Merion Ave, Bryn Mawr, PA 19010-2899; Department of Chemistry, Villanova University, 800 Lancaster Avenue, Villanova, PA 19085-1597; and School of Life Science and Technology, University of Electronic Science and Technology of China, 4 North Jianshe Rd., 2nd Section, Chengdu, China 610054

[*] Corresponding author. E-mail address pbeckman@brynmawr.edu

[*] Corresponding author. E-mail address WangXianlong@uestc.edu.cn

[†]Department of Physics, Bryn Mawr College.

[×]Department of Chemistry, Villanova University.

[§]School of Life Science and Technology, University of Electronic Science and Technology of China.

Abstract

We investigate the *relationship* between intramolecular rotational *dynamics* and molecular and crystal *structure* in 4,4'-dimethoxyoctafluorobiphenyl. The techniques are electronic structure calculations, X-ray diffractometry, and ^{1}H and ^{19}F solid state nuclear magnetic resonance relaxation. We compute and measure barriers for coupled methyl group rotation and methoxy group libration. We compare the structure and the structure-motion relationship in 4,4'-dimethoxyoctafluorobiphenyl with the structure and the structure-motion relationship in related compounds in order to observe trends concerning the competition between intramolecular and intermolecular interactions. The ^{1}H spin-lattice relaxation is nonexponential in *both* the high-temperature short-correlation time limit *and* in the low-temperature long-correlation time limit, albeit for different reasons. The ^{19}F spin-lattice relaxation is nonexponential at low temperatures and it is exponential at high temperatures.

Introduction

The relationship between *structure* and *dynamics* in molecular solids is an ongoing challenge in condensed matter science. Here, we investigate the relationship between intramolecular (rotational) dynamics and molecular and crystal structure in a relatively simple organic solid and model the dynamics in a detailed manner. The compound under investigation, 4,4'-dimethoxyoctafluorobiphenyl (**1**), is, to our knowledge, of no particular interest in and of itself but hopefully, with slow and steady progress, one will be able to perform detailed models like those presented here in more complex and more important systems in the not-too-distant future. In order to arrive at generalities (i.e., for a class of compounds rather than just individual compounds), in the Summary and Conclusions section of this paper we compare the study using **1** presented here with similar studies we have undertaken with 4,4'-dimethoxybiphenyl (**2**)[1,2] and with 3-fluoromethylphenanthrene (**3**).[3,4] We present this summary with as little jargon as possible and we

have attempted to make the presentation in the Summary and Conclusions self-contained. Indeed, the reader not concerned with the details is invited to proceed to that section after reading this Introduction.

1   2   3
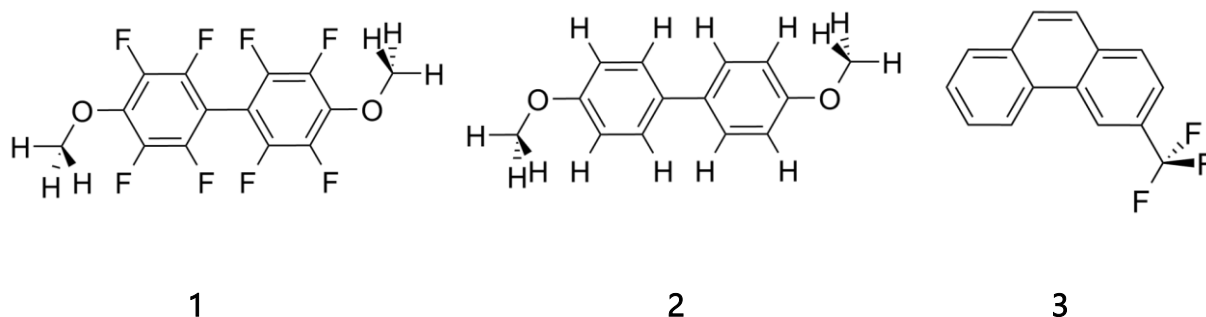
The crystal structure of these compounds is determined by X-ray diffraction,[5] as is the ground state molecular structure in the crystalline environment. The structure of an *isolated* molecule is determined by density functional theory electronic structure calculations. The energies of ground states and transition states for the various rotations (methyl, methoxy, and methoxyphenyl) are calculated. The energy differences between the ground and transition states are the barriers for the rotations. These calculations are done for the isolated molecule and for a central molecule in a suitable cluster of molecules based on the X-ray crystal structure. As such, rotational barriers can be calculated for both the rotations in the isolated molecule and for a molecule in the crystalline environment and the differences in these barriers can provide insight into the relative role played by intramolecular and intermolecular interactions. The calculations in the clusters presumably involve accounting for many van der Waals interactions. Finally, we use solid state ^{1}H and ^{19}F nuclear magnetic resonance (NMR) spin-lattice relaxation experiments[6] to measure activation energies involved with the motions that occur in the crystalline environment. The NMR activation energies are then compared with the electronic structure barrier calculations in the clusters and models for the dynamics are generated.

The NMR relaxation in **1** is complicated. ^{1}H and ^{19}F spin-lattice relaxation occurs because the ^{1}H – ^{1}H and the ^{1}H – ^{19}F dipole-dipole (spin-spin) interactions are modulated by methyl group rotation. The vibrational motions involving the eight ring F atoms are too fast on the NMR time scale to relax the ^{19}F spins and as such ^{19}F – ^{19}F dipole-dipole interactions play no role. The ^{19}F spins can only relax through the methyl ^{1}H spins. The ^{1}H spin-lattice relaxation is nonexponential at all temperatures. At high-temperatures the relaxation is nonexponential because of the 100% correlation among the three H – H vectors as a methyl group rotates.[7,8] The relaxation is nonexponential at low temperatures as a result of ^{1}H – ^{19}F dipolar interactions contributing to the relaxation as well as ^{1}H – ^{1}H dipolar interactions.[3,9] At middle temperatures, *both* phenomena are occurring. Both these phenomena have been observed, but not, to our knowledge, in the same compound. The ^{19}F spin-lattice relaxation is also nonexponential at low temperatures (for the same reason the ^{1}H spin-lattice relaxation is nonexponential) but it is exponential at high temperatures. We are able to fit the temperature dependence of the ^{1}H and ^{19}F relaxation data in a detailed manner with only three adjustable parameters, one of which is an activation energy for methyl group rotation (occurring on the NMR time scale; approximately 10^{-11} s at 280 K to 10^{-7} s at 110 K). The other two parameters that come from fitting the NMR relaxation rate data provide a good test of the Bloch-Redfield-Wangsness model of spin-lattice relaxation[10-12] (which is summarized very clearly by Kimmich[6]) with appropriate modifications[3,7-9] for the two kinds of nonexponential relaxation.

We learn from the electronic structure calculations that methyl group rotation is coupled with the much faster methoxy group libration. We use the term "methyl group rotation" to refer to a rotation from the ground state to a transition state and then back (either in the same rotational sense or in the opposite sense) to the ground state. That is to say, it "rotates over a barrier." We use the term "methoxy group libration" to mean the group rotates from its ground state, part way to its transition state, and then back again. This is a rapid motion occurring on a typical vibration-

libration timescale; say within a few orders of magnitude of 10^{-14} s (which corresponds to a mode of approximately 1000 cm^{-1}).[13]

Various comparisons offer insight into both the intramolecular and the intermolecular interactions involved in these kinds of organic molecular solids as well as insight into the kinds of motions occurring. In **1**, the eight F atoms are on the two rings and the only H atoms are in methyl groups. In **2**, the ring F atoms are replaced with H atoms. We investigate the difference in the structure of the two isolated molecules as a consequence of the larger F atoms in **1**. The two crystal structures are quite different and a comparison provides insight into the competition between intramolecular and intermolecular interactions in going from the isolated molecule to the molecule in the crystal. The methoxyphenyl group (half the molecule) is the asymmetric unit in both crystals of **1** and **2** so this makes these comparisons meaningful. Another interesting comparison involves comparing **1** with **3**. **1** and **3** have the H and F atoms reversed in some sense; **1** has CH$_3$ groups with neighboring F atoms on a ring and **3** has a CF$_3$ group with neighboring H atoms on a ring. There are two major differences, though. One is that the CF$_3$ groups in **3** are bonded directly to the ring and in **1**, the CH$_3$ groups are bonded to an O atom which is then bonded to the ring. Also, in the crystal of **3**, the CF$_3$ groups from different molecules are close enough to each other that *inter*molecular ^{19}F – ^{19}F dipolar interactions matter, in addition to *intra*fluoromethyl ^{19}F – ^{19}F dipolar interactions, in modeling the spin-lattice relaxation, whereas in **1**, the CH$_3$ groups are quite isolated from one another and only the *intra*methyl ^{1}H – ^{1}H dipolar interactions need be considered.

In the solid state, phenyl-phenyl rotation over the barrier in both **1** and **2** is completely quenched but there is coupled methyl group rotation and methoxy group libration in both. The methyl H – ring F interactions (electronic and steric) in **1** are more severe than the methyl H – ring H interactions in **2** and this correlates well with the degree of methoxy group libration (as the methyl group rotates over the barrier). Finally, the NMR activation energy for this coordinated

motion is in excellent agreement with the barriers calculated using electronic structure calculations even though NMR activation energies and barriers calculated by electronic structure calculations are not the same parameter.[14,15] This tends to provide support for both the solid state relaxation NMR and the electronic structure calculation techniques. Determining these low barriers (10 – 20 kJ mol^{-1}) in van der Waals solids using electronic structure calculations is challenging.

Above approximately 80 K in most solids, modeling methyl group rotation as a random hopping of the triangle of H atoms is an excellent model for the interpretation of NMR relaxation data.[16-24] This is the model of methyl group rotation used here. Below approximately 80 K in most solids, methyl group rotation is better described by quantum mechanical tunneling. The transition from the low-temperature quantum mechanical tunneling regime to the high-temperature semiclassical hopping regime is well understood.[16-18,20,23,25]

Experimental Methods

X-ray Crystallography. The sample of compound **1**, 4,4'-dimethoxyoctafluorobiphenyl, (99%, mp 85-88°C) was purchased from Acros. The crystal structure was determined by X-ray crystallography[5] at both 100 and 200 K. At 100(2) K, a single colorless block (0.44 X 0.28 X 0.26 mm) was mounted, using Paratone$^®$ oil, onto a glass fiber and cooled to the data collection temperature. Data were collected on a Brüker-AXS Kappa APEX II CCD diffractometer with 1.54178 Å Cu-Kα radiation. Unit cell parameters were obtained from 90 data frames, 0.3^O Φ, from three different sections of the Ewald sphere yielding $a = 13.1644(5)$, $b = 7.7256(3)$, $c = 12.5307(5)$ Å, $V = 1274.4(1)$ Å^3. 4613 reflections ($R_{int} = 0.0182$) were collected (1115 unique) over $\theta = 6.64^O$ to 67.54^O. The systematic absences in the diffraction data were consistent with the centrosymmetric, orthorhombic space group, *Pbcn*. The data-set was treated with SADABS (Sheldrick, G., Brüker-AXS, 2001) absorption corrections based on redundant multi-scan data. $T_{max}/T_{min} = 1.28$. All non-hydrogen atoms were refined with anisotropic displacement parameters.

All hydrogen atoms were treated as idealized contributions. The goodness of fit on F^2 was 1.070 with $R1$($wR2$) 0.0309(0.0940) for [$I_q > 2(I)$]. The largest difference peak was 0.238 e/Å^3 and the largest difference hole was –0.229 e/Å^3.

At 200(2) K, the single colorless block was (0.23 X 0.21 X 0.09 mm) and the unit cell is characterized by a = 13.1708(4), b = 7.8476(2), c = 12.6056(4) Å, V = 1302.90(7) Å^3. 3645 reflections (R_{int} = 0.0345) were collected (1128 unique) over θ = 6.57 to 67.99^O. T_{max}/T_{min} = 1.24 and the goodness of fit on F^2 was 1.085 with $R1$($wR2$) 0.0491(0.1329) for [$Iq>2(I)$]. The largest difference peak was 0.310 e/Å^3 and the largest difference hole was –0.329 e/Å^3.

The structure of the molecule in the solid state is shown in Figure 1(a) (which also shows the carbon numbering) and the crystal structure is shown in Figures 1(b and c). The differences in structure between 100 K and 200 K are not visible at the resolution of Figure 1.

Electronic Structure Calculations in the Isolated Molecule. All electronic structure calculations were carried out with the Gaussian 03 package of programs.[26] Similar computational schemes have been used to study the internal rotation motions of **2**[2] and **3**.[4] An isolated molecule of **1** was taken from the X-ray crystallographic structure. To obtain the ground state, a full geometry optimization was performed at the B3LYP/6-311+G(d,p) level to reach the local energy minimum.[27-32] There are three kinds of internal rotational degrees of freedom in the molecule: phenyl-phenyl rotation around the C1–C1' bond, methoxy group rotation around the O–C4 bond, and methyl group rotation around the Cm–O bond. Here, the letter "m" refers to the methyl carbon atom. Carbon numbering is indicated in Figure 1. Dihedral angles γ (C6–C1–C1'–C2'), δ (Cm–O–C4–C5), and α (H–Cm–O–C4) are used as the rotational coordinates of the whole 4-methoxytetrafluorophenyl group, the 4-methoxy group, and the methyl group, respectively. Potential energy surfaces for the three kinds of rotations were obtained at the B3LYP/6–311+G(d,p)//B3LYP/6–311+G(d,p) level by scanning γ, δ, and α from 0° to 180° at intervals of 15°. Calculations were performed with the respective dihedral angle fixed while

allowing all other structural parameters to be optimized. Additional points were calculated around the transition states. Previous experience shows this computational scheme is a reasonable compromise between the accuracy and speed in studying the internal rotation problem.[2,4] The ground state and transition state identified through this scheme were indistinguishable from those obtained directly from locating the minimum and first-degree saddle points.[4,33]

Electronic Structure Calculations in a Cluster. A cluster consisting of 19 molecules of **1** was constructed from the single-crystal X-ray crystallographic structure of the compound. The cluster is shown in Figures 1(b and c). The environment of the central molecule in the cluster was intended to simulate the crystal packing interactions as experienced by a molecule in an ideal crystal. The cluster fixes all C, O, and F atoms at their positions as determined in the X-ray structure for the ground state, while the positions of H atoms in all states were determined by the electronic structure calculations at the B3LYP/6−31G(d) level. This is important because the X-ray experiments position the hydrogen atoms with C−H bond lengths that are too short.[34,35] For example, the X-ray positioning of the H atoms (placed in idealized positions) in **1** gives the methyl C−H bond lengths as 0.98 Å whereas the calculations give these bond lengths as 1.076, 1.078, and 1.080 Å, a difference of approximately 0.10 Å, consistent with previous studies.[34,35] The shortening can be as large as 0.03 Å for C−H bond lengths in methyl groups as determined by neutron diffraction measurements at room temperature (due to thermal vibrations).[35] Determining H atom positions accurately is important because the H−H distances in a methyl group r enter into the calculation of an important NMR parameter as r^{-6}. This is discussed below.

Potential energy surfaces were calculated for the internal rotations on the central molecule of the cluster. Prior experience shows that the cluster is large enough that all neighboring molecules with significant intermolecular interactions with the central molecule have been included and adding more neighboring molecules would not significantly change the calculated barriers.[4,33,36] Due to the high computational cost, the basis set superposition error, which has been

shown not to be significant for the calculation of rotational barriers,[4] was not corrected.

Two groups of calculations, all at the B3LYP/6-31G(d) level, were performed. In the *rigid rotation model*, calculations were done for 15º steps in γ, δ, and α. The rotational ground and transition states of the methyl group identified from these calculations were subject to an additional *partial relaxation* calculation. In the *partial relaxation* model, all structural parameters of the central molecule were allowed to optimize except that the Cartesian coordinates of carbons at 1, 1', 4 and 4' positions were fixed. Previous studies have shown that the barriers obtained from the partial relaxation models are comparable with the rotational activation energy as measured by solid state NMR relaxation experiments.[2,4,33,36]

Rotational barriers were taken to be the difference in the calculated energies between the ground and transition states for methyl group rotation, methoxy group rotation, and 4-methoxytetrafluorophenyl group rotation.

Solid State [1]H Spin-lattice Relaxation Experiments. [1]H and ^{19}F spin-lattice relaxation measurements in a polycrystalline sample of **1** were made between 110 and 280 K at an NMR frequency of 22.5 MHz. The experiments with the two spin species are fixed frequency, *not* fixed magnetic field. When the magnetic field is 0.527 T, the ^{1}H NMR frequency is $w_H/2\pi = 22.5$ MHz (^{1}H observed) and the ^{19}F NMR frequency is $\omega_F/2\pi = 23.9$ MHz ([19]F *not* observed). When the magnetic field is 0.560 T, the ^{19}F NMR frequency is $w_F/2\pi = 22.5$ MHz (^{19}F observed) and the ^{1}H NMR frequency is $w_H/2\pi = 21.2$ MHz ([1]H *not* observed). Temperature control and measurement is discussed in detail elsewhere.[1] [1]H or ^{19}F magnetization recovery curves were measured using an inversion-recovery pulse sequence. It is convenient to define three temperature regions: a high-temperature region I, $154 < T < 286$ K ($3.5 < 10^3/T < 6.5$ K^{-1}), a middle temperature region II, $133 < T < 154$ K ($6.5 < 10^3/T < 7.5$ K^{-1}), and a low-temperature region III, $114 < T < 133$ K ($7.5 < 10^3/T < 8.8$ K^{-1}).

Nonexponential ^{1}H spin-lattice relaxation was observed at *all* temperatures and nonexponential ^{19}F spin-lattice relaxation was observed in the low-temperature region III. Exponential ^{19}F relaxation was observed in the high-temperature region I and in the middle temperature region II and in those regions ^{19}F magnetization recovery curves were fitted to a single exponential $M_F(t) = M_F(\infty)[1-(1-\cos\theta)\exp(-\lambda_2 t)]$. λ_2 is the nuclear spin-lattice relaxation rate, $M_F(\infty)$ is the equilibrium ^{19}F magnetization, and the adjustable parameter θ accounts for imperfections in the perturbing inversion π-pulse. The nonexponential ^{19}F and ^{1}H relaxation in the low temperature region III was fitted with a double exponential $M_k(t) = M_{k1}(\infty)[1-(1-\cos\theta)\exp(-\lambda_1 t)] + M_{k2}(\infty)[1-(1-\cos\theta)\exp(-\lambda_2 t)]$ (with k = H, F for ^{1}H or ^{19}F). The two relaxation rates in this case are λ_1 and λ_2. Figure 2 shows an example of a ^{1}H magnetization decay in the low-temperature regime III where the double exponential fits the data. Figure 3 shows an example of a ^{1}H magnetization decay in the high-temperature region I where a double exponential does *not* fit the data (as expected and as discussed in the next section). This is the case for the ^{1}H magnetization decay in the middle temperature region II as well. Both Figures 2 and 3 show a fit to a single exponential for comparison. Figure 3(d) shows a single exponential fit to the initial part of the nonexponential recovery curve in the high temperature region I, in which case the rate is λ_1. We expand on the procedure used to determine this initial rate elsewhere.[1] Figure 4 shows the temperature dependence of these relaxation rates and is discussed more fully in the next section. The two fractional magnetizations $\phi_{H1} = M_{H1}(\infty)/[M_{H1}(\infty) + M_{H2}(\infty)]$ and $\phi_{H2} = M_{H2}(\infty)/[M_{H1}(\infty) + M_{H2}(\infty)]$ characterizing the ^{1}H double exponential relaxation in the low temperature region III (and discussed further in the next section) are shown in Figure 5. (Figure 5 also shows the failed attempts to fit the ^{1}H magnetization decays to a double exponential in the middle temperature region II.)

The NMR Relaxation Model and the NMR Parameters

The 4,4'-dimethoxyoctafluorobiphenyl molecule **1** has two identical halves; each with four ring F atoms and three H atoms in a methyl group. An analysis (in the NMR Relaxation Results section below) of the parameters determined by fitting the NMR relaxation rates in **1** shows that the principle motion causing the ^{1}H spin-lattice relaxation is methyl group rotation. On the NMR timescale, the F and H atom vibrations and the methoxy group libration are too fast to cause nuclear spin relaxation. The methyl group, on the other hand, reorients with a temperature-dependent mean hopping frequency in resonance with the NMR frequency in the temperature range studied. Indeed, the ability to isolate a single motion in this fashion renders nuclear magnetic resonance relaxation studies potentially very powerful. We first briefly review the basic Bloch-Wangsness-Redfield model for nuclear spin-lattice relaxation[10-12] (which is summarized in the texts by Abragam,[9] Slichter,[37] Ernst *et al.*,[38] and Kimmich[6]) and then extend it two ways; first to include the fact that there are two spin species and second to include cross correlation effects involving the three H atoms in a methyl group. The ^{1}H relaxation is nonexponential at all temperatures so the goal is to determine an appropriate rate or rates from the nonexponential relaxation that correspond to the basic Bloch-Wangsness-Redfield model. Appropriate ^{19}F rates must also be extracted from the basic model. (The ^{19}F spins can only relax by trading energy with the ^{1}H spins.)

The *basic* [1]H relaxation rate in the Bloch-Wangsness-Redfield model for a polycrystalline powder is

$$R = C\left[J\left(w_{\mathrm{H}}, t\right) + 4J\left(2w_{\mathrm{H}}, t\right)\right], \tag{1}$$

where $w_{\mathrm{H}}/2\pi$ is the ^{1}H NMR frequency. The spectral density for random motion described by Poisson statistics in eq 1 is

$$J(w, t) \; = \; \frac{2\,t}{1 + w^2\,t^2} \tag{2}$$

and the mean time between methyl group hops is[16-25]

$$t \; = \; t_{\infty}\,e^{E_{\mathrm{NMR}}/kT}. \tag{3}$$

where E_{NMR} is the "NMR activation energy." It is convenient to scale the infinite temperature mean time between hops t_{∞} (which is an experimental fitting parameter) by a very simple harmonic model[39]

$$\tilde{t}_{\infty} \; = \; \left(\frac{2\,\rho}{3} \right) \left(\frac{I}{2E_{\mathrm{NMR}}} \right)^{1/2} , \tag{4}$$

where I is the moment of inertia of the methyl group. A fitted value of t_{∞} that subsequently results in a value of $t_{\infty}/\tilde{t}_{\infty}$ several orders of magnitude from unity would suggest the motion is not methyl group rotation.

The NMR relaxation parameter C in equation 1 is a measure of all the $^{1}\mathrm{H} - {}^{1}\mathrm{H}$ spin – spin dipolar interactions, both intramolecular (i.e. intramethyl) and intermolecular (i.e., intermethyl), being modulated by methyl group rotation. It involves a sum over all pairwise interactions. It is both the changing *lengths* and the changing *directions* of the spin-spin vectors that cause the spin-lattice relaxation. The *distances* between the three H atoms r_{HH} in a methyl group are time independent and are known to high precision from the electronic structure calculations as discussed previously in this paper. This intramethyl contribution to C resulting from the 120° changes in direction of the intramethyl H – H vectors as the methyl group hops is labeled $\tilde{C}$ and is given by

$$\tilde{C} = \left(\frac{9}{40}\right)\left(\frac{\mu_o}{4\pi}\right)^2\left(\frac{\hbar\gamma_H^2}{r_{HH}^3}\right)^2. \tag{5}$$

The parameter γ_H is the ^{1}H magnetogyric ratio and m_o is the magnetic constant. $\tilde{C}$ can be calculated explicitly and $C/\tilde{C}$ is often taken as a fitting parameter, though in this study we will set $C = \tilde{C}$ as discussed later in this section.

Both the ^{1}H and ^{19}F relaxation in the low-temperature region (region III in Figure 4) is nonexponential because the two spin species interact with one another via the unlike spin dipole-dipole interaction. We have provided a brief review of the literature related to this phenomenon.[3] Although the [1]H – [19]F interactions play a role at all temperatures, both spin species relax exponentially in temperature regions I and II (if this were the only phenomenon occurring). This is discussed further below. A recent work[40] nicely summarizes the various interactions that ^{19}F spins can be involved with for a liquid crystal with many kinds of motions – some of them quite slow – and shows why, at 22.5 MHz in a polycrystalline powder, we are not concerned with the spin rotation or chemical shift interactions for either ^{1}H or ^{19}F relaxation. The NMR frequencies for ^{1}H and ^{19}F are close enough that, with a little help from the thermal bath of phonons, mutual spin flips can occur via the [1]H – [19]F interactions. As such, the "mobile" [1]H spins in the methyl groups can relax the "immobile" [19]F spins. The result is that the two macroscopic magnetizations (i.e., $M_H(t)$ associated with the ^{1}H spin species and $M_F(t)$ associated with the ^{19}F spin species) form a two-component vector and the time dependence of the recovery of these two magnetizations following a perturbation is related to the two equilibrium magnetizations via:[3]

$$\frac{d}{dt}\begin{bmatrix} M_H(\infty) - M_H(t) \\ M_F(\infty) - M_F(t) \end{bmatrix} = -\begin{bmatrix} R_{HH}^L & 0 \\ 0 & R_{FF}^L \end{bmatrix} + \begin{bmatrix} R_{HH}^U & R_{HF}^U \\ R_{FH}^U & R_{FF}^U \end{bmatrix}\begin{bmatrix} M_H(\infty) - M_H(t) \\ M_F(\infty) - M_F(t) \end{bmatrix}. \tag{6}$$

Eq 6 is constructed so the first term corresponds to the relaxation rates that would be observed if there were no $^1\text{H} - {}^{19}\text{F}$ dipolar interactions in which case the relaxation of the perturbed ^1H or ^{19}F magnetizations are completely decoupled and each relaxes exponentially. R_{HH}^{L} (where the superscript L means "like" as in "like spins") in the first diagonal matrix in given by eqs 1-3 and 5. $R_{\text{FF}}^{\text{L}} = 0$ zero since no $^{19}\text{F} - {}^{19}\text{F}$ dipolar interactions are modulated on the NMR time scale. The second matrix (where the superscript U means "unlike" as in "unlike spins") accounts for the $^1\text{H} - {}^{19}\text{F}$ dipolar interactions. Although $R_{\text{FF}}^{\text{L}} = 0$ in the first matrix of eq 6, all four entries R_{HH}^{U}, R_{FF}^{U}, R_{HF}^{U}, and R_{FH}^{U} in the second matrix are non zero and expressions for them can be found in reference 3. They can all be determined using logical extensions of the basic Bloch-Wangsness-Redfield model. Instead of equations like eq 1, the spectral densities $J(w_{\text{H}} + w_{\text{F}}, t)$ and $J(w_{\text{H}} - w_{\text{F}}, t)$ are involved, in addition to $J(w_{\text{H}}, t)$ and $J(2w_{\text{H}}, t)$. The spectral densities $J(w_{\text{F}}, t)$ and $J(2w_{\text{F}}, t)$ do *not* appear. The four multipliers corresponding to C in eq 1 involve the ^{19}F gyromagnetic ratio g_{F} (as well as g_{H}) and the F-H atom distances r_{FH}.[3]

Eq 6 means that the nuclear magnetizations $M_{\text{H}}(t)$ and $M_{\text{F}}(t)$ both relax with two time constants λ_1 and λ_2 via;

$$\frac{M_k(\yen) - M_k(t)}{2 M_k(\yen)} = f_{k1}\, e^{-\lambda_1 t} + f_{k2}\, e^{-\lambda_2 t}, \qquad (7)$$

for $k = \text{H, F}$. The factor 2 is solely for convenience for the case of a perturbation using a p-pulse. The normalized magnetizations f_{k1} and f_{k2} depend on the initial conditions (i.e., on $M_k(0)$) but *the observed relaxation rates λ_1 and λ_2 do not.* The rates λ_1 and λ_2, are obtained by diagonalizing the relaxation matrix in eq 6 and are

$$l_{1,2} = \frac{1}{2}\left[\left(R_{FF}^L + R_{FF}^U\right) + \left(R_{HH}^L + R_{HH}^U\right) \pm \sqrt{\left[\left(R_{FF}^L + R_{FF}^U\right) - \left(R_{HH}^L + R_{HH}^U\right)\right]^2 + 4 R_{FH}^U R_{HF}^U}\right], \quad (8)$$

(with $R_{FF}^L = 0$ in the present case). Eq 8, then, relates the observed λ_1 and λ_2, to the relaxation rates determined from the basic Bloch-Wangsness-Redfield model. If the ^{1}H spins are being observed and a p-pulse inverts the ^{1}H magnetization (i.e., $M_H(0) = - M_H(\yen)$), the amplitudes of the observed normalized magnetization in eq 7 are[3]

$$f_{H1} = 1 - f_{H2} = \frac{R_{HH}^L + R_{HH}^U - l_2}{l_1 - l_2}. \qquad (9)$$

Experimental values of f_{H1} and f_{H2} are plotted in Figure 5. If the ^{19}F spins are being observed and a p-pulse is applied to the ^{19}F magnetization then all the Hs in eq 9 are replaced with Fs. Both spin species relax with the *same* two spin-lattice relaxation rates λ_1 and λ_2, *regardless* of the relative numbers of spins in each species and the number of mobile and immobile atoms of each spin species. The fractional magnetizations in eq 9 each approach 0.5 at low temperature. As temperature is increased one of these approaches 1 and the other approaches 0 as observed (Figure 5). Thus, even though the relaxation is inherently nonexponential at higher temperatures (regions I and II), one magnetization disappears and only the other one is observed. As such, discounting other phenomenon (discussed below), the *observed* relaxation is exponential at higher temperatures: The ^{1}H magnetization relaxes with λ_1, which is observed when the ^{1}H magnetization is observed, and the ^{19}F magnetization relaxes with λ_2, which is observed when the ^{19}F magnetization is observed. Further details are provided elsewhere.[3] The two maxima in Figure 4 are predicted by this model. The maximum at approximately $10^3 T^{-1} = 6.2$ K^{-1} occurs when $\omega_F \approx$

$\omega_H \approx \tau^{-1}$ and the maximum at approximately $10^3\,T^{-1} = 7.7\,K^{-1}$ occurs when $\omega_F - \omega_H \approx \tau^{-1}$. Despite all these complexities, there is only a single motion (methyl group rotation) and eqs 2 and 3 are valid throughout the entire analysis. All this complexity results in one additional parameter, q, that is presented below.

Whereas the recovery of the ^{19}F magnetization in **1** is found to be exponential at higher temperatures as presented above, there is an *additional* phenomenon, *unrelated* to the effects discussed in the previous paragraphs, for the ^{1}H magnetization recovery at higher temperatures (regions I and II) which *also* results in nonexponential relaxation. The basic Bloch-Redfield-Wangsness model used here assumes the existence of [1]H – [1]H pairs whose internuclear vectors are reorienting randomly. The pairs are not interacting with each other and their motion is uncorrelated. Extending this to the three ^{1}H spins in a methyl group while keeping these assumptions is straightforward and results in the factor 9/40 in eq 5. However, the reorientation of the three spin-spin vectors in a methyl group is *neither* random *nor* uncorrelated. First, each triangle of spins reorients in a plane, not isotropically. (Albeit, because of rapid methoxy group libration as discussed below, this plane is not fixed in space but librates with the methoxy group. This methyl group plane libration is too fast to mask the effects being discussed here.) Second, the motion of the three spin-spin vectors are 100% correlated. Runnels[7] and Hilt and Hubbard[8] dealt with these complications in great detail and the results are discussed elsewhere.[1] For a polycrystalline sample, the magnetization recovery after a perturbation cannot be modeled in a simple closed form.[8] We show in Figure 3 that not even a double exponential will fit the data. In this case, however, the single unique relaxation rate λ_1, related to the basic Bloch-Redfield-Wangsness model as outlined above, corresponds to the *initial exponential recovery* of the magnetization in the nonexponential relaxation. The experimental analysis of high-temperature nonexponential relaxation for the three ^{1}H spins in a methyl group leading to the determination of this initial rate is presented elsewhere.[1]

To summarize, the ^{1}H relaxation is nonexponential at high and low temperatures for completely different reasons; two unrelated phenomena are at work. At middle temperatures (region II), both mechanisms are at work and interpreting the ^{1}H spin-lattice relaxation rate data is complicated as discussed below. Despite the complexities associated with both nonexponential spin-lattice relaxation and the presence of two spin species, there are only five independent parameters in the *model* that characterizes both the ^{1}H and ^{19}F spin-lattice relaxation over all three temperature regions. Here, we set two of these parameters to their theoretically computed values, leaving only *three* adjustable (fitting) parameters. Fixing two parameters at their theoretical values (or, seen another way, eliminating them as adjustable parameters), is based on the crystal structure. (1) Since the only hydrogen atoms are in methyl groups, and since the methyl groups are relatively far apart, the only ^{1}H spin –^{1}H spin interactions that need be considered are those that characterize the intramethyl ^{1}H spin –^{1}H spin interactions. In this case, C in eq 1 is set to $\tilde{C}$ in eq 5. It is important, however, to use the correct H – H distance, r_{HH}, in a methyl group. Since $\tilde{C}$ is proportional to r_{HH}^{-6}, a given % error in r_{HH} results in six times this % error in $\tilde{C}$. (2) In the 2 X 2 relaxation matrix introduced above, there are several other constants[3] and they can be related to $\tilde{C}$ and therefore computed explicitly. The only one that cannot be calculated explicitly is one that characterizes an average overall ^{1}H (methyl) spin – ^{19}F (ring) spin interaction. This average interaction is characterized by the interaction constant $q\tilde{C}$ where q is a dimensionless number and should be much less than 1 if the model is to make any sense. It can be thought of, conceptually, as a ratio: the average of the strengths of the ^{1}H (methyl) spin – ^{19}F (ring) spin interactions (both intramolecular and intermolecular), divided by the strength of the intramethyl ^{1}H spin – ^{1}H spin interactions. It is primarily, but not completely, the dependence of the ^{1}H – ^{19}F interaction strengths on the H – F distances r_{FH}^{-6} that makes q small. The time dependence of the *direction* of the spin-spin vectors (relative to the applied magnetic field) also plays a role. The angular variations of the various vectors $\vec{r}_{FH}$ tend to be small. (3) There is another term that characterizes

the *inter*methyl ^{1}H spin $-$ ^{1}H spin interactions and this term[3] is set to zero for **1** since the methyl groups are relatively far apart (and, again the r_{HH}^{-6} dependence of the interactions plays a role). (4) An NMR activation energy E_{NMR} for methyl group rotation and (5) a preexponential factor τ_∞ in eq 3 are used to model the mean time between methyl group hops τ. It is convenient to fit with $\tau_\infty / \tilde{t}_\infty$ using eq 4. For **1**, then, there are only three adjustable parameters; E_{NMR}, $\tau_\infty / \tilde{t}_\infty$, and q.

Results

Single-crystal X-ray diffraction. The crystal structure of 4,4'-dimethoxyoctafluorobiphenyl (**1**) at 200 K is shown in Figures 1(b and c). At the resolution of the Figure, the structure is the same at 100 K. Although there are 4 molecules per unit cell ($Z = 4$), there is a great deal of symmetry and the asymmetric unit is half a molecule ($Z' = ½$). This means that all methyl (and methoxy and phenyl) groups are chemically equivalent. Figure 1(a) shows a single molecule taken from the crystal structure in Figure 1(b and c) by eliminating all but one molecule in Figure 1(b and c). The methyl carbon thermal ellipsoids (not shown) show elongation perpendicular to the ring plane (compared with the ring carbons) and this correlates well with the methoxy group libration discussed below. Characteristic bond lengths and bond angles for the molecular structure observed at both 100 and 200 K are given in Table 1. The root mean square deviation between the two sets of bond lengths (100 and 200 K) is 0.003 Å, meaning that to within the experimental uncertainties in bond lengths the two structures are identical. The differences in the various angles are also negligible. Whereas there is no difference in the molecular structures at the two temperatures, the volume of the unit cell is 2.2 ± 0.2 % larger at 200 K than it is at 100 K. This corresponds to an average volume coefficient of thermal expansion of $(2.2 \pm 0.2) \times 10^{-4}$ K^{-1} or, what is more relevant for the calculations performed here, an average linear coefficient of thermal expansion of $(7.4 \pm 0.8) \times 10^{-5}$ K^{-1}. This thermal expansion is small enough that the

changes in the intermolecular van der Waals interactions over the temperature range studied will be very small. These interactions are important for the electronic structure calculations.

Electronic Structure Calculations in the Isolated Molecule. The isolated molecule structure of **1** is similar to the structure of the molecule in the crystal as determined by X-ray diffraction. In Table 1, we show the comparison of the major structural parameters between the calculated values for the isolated molecule and the X-ray values for the molecule in the crystal. The electronic structure calculations for an isolated molecule reproduce the bond lengths, bond angles and most bond dihedral angles found in the molecule in the crystal. The greatest difference lies in the dihedral angles formed between the two fluoro-substituted phenyl rings (γ) and between the 4-methoxy group and the phenyl ring (δ). The dihedral angle between the two phenyl rings, γ (C6–C1–C1'–C2'), has a minimum at -62.5^O (the negative sign reflects the handedness of the angle). In the X-ray crystal structure, this dihedral angle is slightly smaller, -58.0^O. The dihedral angle between the methoxy group and the phenyl ring, δ (Cm–O–C4–C5), is 40.0^O in the calculated isolated molecule structure while in the molecule in the crystal as determined by X-ray diffraction, this value is 13.3^O. These differences reflect the competition between non-bonded intramolecular interactions and intermolecular interactions in the crystal packing environment.

Interconversion between the ground state conformations at $\gamma = -62.5^O$ (presented above) and an equivalent ground state at $\gamma = -117.5^O$ (noting that $117.5^O + 62.5^O = 180^O$) for the rotation of the two 4-methoxytetrafluorophenyl groups relative to each other needs to cross over a transition state at $\gamma = -90°$, i.e. the two phenyl rings perpendicular to each other. This transition state has a very low potential energy of 1.6 kJ mol^{-1} relative to the ground state. However, for the other rotational route that crosses the co-planar conformation for the phenyl rings, there are barriers of 64.7 kJ mol^{-1} at $\gamma = 0^O$ and 70.4 kJ mol^{-1} at $\gamma = 180^O$. In the $\gamma = 0^O$ transition state the 4-methoxy group and the 4'-methoxy group are in a trans configuration and in the $\gamma = 180°$ transition state the 4-methoxy group and the 4'-methoxy group are in a cis configuration. Even so, the two

phenyl rings are *not* coplanar in these transition states. Instead, the (improper) dihedral angles C1−C2−C6−C1' and C1'−C2'−C6'−C1 are twisted out of the planar configuration by about 25° to 155° (from 180°) to avoid the close contacts between F atoms.

The potential energy surface for the 4-methoxy group rotation shows a pseudo 4-fold symmetry (the four conformations with the methoxy group perpendicular and coplanar with the phenyl ring are all rotational transition states) and the rotational barrier is small; approximately 1.3 kJ mol^{-1}. Methyl group rotation shows a common 3-fold energy profile, in which the transition state is the conformation with one Cm−H bond eclipsed with the O−C4 bond. The barrier is 4.1 kJ mol^{-1}. In the transition state for the methyl group rotation, the methoxy group reorients by 17° from $\delta = 40^O$ to 57°.

Electronic Structure Calculations in the Cluster. In the *rigid rotation model*, potential energy surfaces for the rotation of the methoxy group and the rotation of the methyl group in the central molecule of the cluster [Figures 1(a and b)] were calculated for $0^O < \delta < 180^O$ and $0^O < \alpha < 180^O$ in 15° steps, respectively. Potential energy surfaces for the 4-methoxytetrafluorophenyl group rotation and 1,4-tetrafluorophenlyene group rotation were calculated for $-88^O < \gamma < -28^O$ ($\pm30^O$ around the thermal equilibrium value of $\gamma = -58^O$ found in the crystal) in 5° steps. For the rotation of the substituted benzene ring alone (1,4-tetrafluorophenlyene group) or the 4-methoxytetrafluorophenyl group around the C1−C1' bond, the energy has already gone up more than 170 kJ mol^{-1} when the dihedral angle γ is 30° away from its thermal equilibrium value of -58°. In addition, the barrier height for the methoxy group is approximately 340 kJ mol^{-1}. *Therefore, we may conclude that the rotation of the methoxy group or the substituted phenyl group over their barriers is completely quenched in the crystal.* For the methyl groups, the staggered conformation ($\alpha = 54^O$) in the ground state is found in the optimized structure of the central molecule in the cluster. The barrier height for the methyl group rotation in this rigid rotation model (α: $54^O \rightarrow 0^O$) is 25.5 kJ mol^{-1}.

In the *partial relaxation model*, all the structural parameters of the central molecule were allowed to optimize except that C1, C1', C4 and C4' were held at their crystallographically measured positions. The barrier height for methyl group rotation becomes 17.1 kJ mol^{-1}. In the optimized ground state structure, the two phenyl groups form a dihedral angle of $\gamma \approx -55^O$ which is very close to the value -58° found in the X-ray crystal structure; the orientation of the methoxy group is also nearly identical to that found in the crystal structure, $\delta \approx 14^O$ vs. $\delta \approx 13^O$ in the crystal. These results show from another perspective that the cluster is a reasonable model for the molecule in the crystal packing environment and that the intermolecular interactions have been properly accounted for in the electronic structure calculations. In the transition state for the methyl group rotation, in which one of the C–H bonds is eclipsed with the O–C4 bond, the most significant changes are that the methoxy group reorients by 29° from $\delta = 13^O$ to 42°. Such structural libration significantly relieves the repulsion between an H atom and the F atom at the 3-position.

NMR relaxation. In both the high-temperature region I and the middle temperature region II (Figure 4), the ^{19}F spin-lattice relaxation is exponential and λ_2 is the relaxation rate. In the high temperature region I and in the middle temperature region II the ^{1}H spin-lattice relaxation is nonexponential (and *not* fitted by a double exponential as indicated in Figures 3 and 5). The meaningful ^{1}H relaxation rate is the one that describes the short-time recovery of the magnetization and can be interpreted as the theoretical rate λ_1. Both the ^{1}H and ^{19}F relaxation curves in the low-temperature region III in Figure 4 require (and are well-fitted by) double exponential fits (Figure 2) and *both* spin species relax with *both* λ_1 and λ_2 as indicated in Figure 4. There are three adjustable parameters; E_{NMR}, $\tau_\infty / \check{\tau}_\infty$, and q. The double lines in region III of Figure 4 are a consequence of the fact that the experiments for the two spin species were performed at the same NMR frequency, not the same magnetic field.[3] First, $E_{NMR} = 16.5 \pm 1.7$ kJ mol^{-1} in eq 3 is the NMR activation energy for methyl group rotation. Although all three parameters are obtained from a global fit,

conceptually, one can think of E_{NMR} as being determined by the slope of $\ln\lambda_1$ and $\ln\lambda_2$ versus T^{-1} at both high and low temperatures. Second, τ_∞ is the preexponential factor in the Arrhenius relation eq 3. One can think of changing τ_∞ as moving relaxation curves in Figure 4 left and right (i.e., to higher and lower inverse temperature). The global fit gives $\tau_\infty / \tilde{t}_\infty = 0.3 \pm 0.2$. The third parameter is the single parameter q that characterizes the $^1H - {}^{19}F$ cross-relaxation[3] and the fit shown in Figure 4 gives $q = 0.020 \pm 0.005$. With the other parameters held constant, q is related to the difference $\lambda_1 - \lambda_2$. If $q = 0$, all cross couplings would be zero, the ^1H relaxation would be exponential at low temperatures and the ^{19}F relaxation rate would be zero at all temperatures (i.e., no relaxation) since the F atoms are not moving on the NMR timescale. So, q is small but it cannot be taken to be zero as an approximation.

Summary and Conclusions

We present a summary and a series of conclusions arrived at by comparing (a) X-ray diffraction experiments, (b) density functional theory electronic structure calculations in both isolated molecules and in molecules in the crystalline environment, and (c) NMR ^1H and ^{19}F spin-lattice relaxation experiments in 4,4'-dimethoxyoctafluorobiphenyl (**1**) (presented here), 4,4'-dimethoxybiphenyl (**2**) (presented elsewhere [1,2]), and 3-fluoromethylphenanthrene (**3**) (also presented elsewhere[3,4]). We investigate and compare the differences in the ground state structures of **1** and **2** both in the isolated molecule and in the crystal. The structure of a molecule of **3** (which has no internal rotation axes other than that of the fluoromethyl group) is essentially the same in both the isolated molecule and in the crystal. Compound **1** has two OCH_3 groups and eight ring F atoms. Compound **2** has two OCH_3 groups and eight ring H atoms.

(1) The angle between the two rings is 40° in the isolated molecule of **2** while the two rings are coplanar (i.e., 0°) in the crystal. The repulsion between H atoms at the 6 and 2' positions and between H atoms at the 2 and 6' positions pushes the two rings away from each other to form this

angle of 40º. (See Figure 1 for atom labeling, which is the same for compounds **1** and **2**.) The intramolecular energy cost to force them to be coplanar in the solid in **2** is 8 kJ mol^{-1}. This energy is provided by the intermolecular interactions in the crystal which results in a coplanar conformation and an overall lower total intramolecular plus intermolecular energy. In an isolated molecule of **1**, greater repulsion between F atoms at the 6 and 2' positions and at the 2 and 6' positions causes the phenyl rings to twist to 62.5^O. Forcing them to be coplanar costs at least 65 kJ mol^{-1}. This energy cost is too large for intermolecular interactions in the crystal to compensate for and as a result this angle decreases by only 4.5^O to 58.0^O in the solid.

(2) In crystals of both **1** and **2**, the asymmetric unit is half a molecule. Having dealt with the angle between the two halves above, we now only have to consider half the molecule in both the isolated molecule and the molecule in the crystal in discussing the structure of the ground state for the methoxy and methyl groups. In an isolated molecule of **2**, the dihedral angle Cm–O–C4–C5 (the methoxy group angle) is 0° (meaning that the methoxy group lies in the plane of the ring). This angle increases to only 3° in the crystal; a small change. But in **1**, the F atoms at the 3 and 5 positions provide a strong repulsion to the 4-methoxy group. The methoxy group is oriented 40° out of the plane in the isolated molecule and, in the crystal, this is lowered to 13° as a consequence of intermolecular interactions.

(3) For the electronic structure calculations, the C and O positions in a suitable cluster of molecules is taken from the X-ray diffraction studies. It is important, however, to allow the positions for some C and O atoms to relax in the transition state (i.e., change from the positions determined by X-ray diffraction). Indeed, if this is not done, the computed barrier for methyl group rotation (or methyl group rotation plus methoxy group libration) is considerably too large. The difference between the total energy in the ground state and the total energy in the transition state is taken as the barrier for the particular rotation. (The determination of the positions of the H atoms in general, and the positions of the fluoromethyl F atoms in **3** are discussed below.)

(4) Compound **3** involves "simple" fluoromethyl group rotation. However, in **1** and **2**, the coupling between the methyl group and the methoxy group potential energy surfaces (determined by electronic structure calculations) suggests a coupled motion: methyl group rotation (through a transition state) and methoxy group libration (a rotation part way to a transition state and back again). Strictly speaking, however, the calculations say nothing about motion. The calculations just provide a two-dimensional energy surface. A model for the "motion" involves the moments of inertia of the rotating groups and other assumptions and approximations. The methoxy group libration will be much faster than the methyl group rotation as discussed in the Introduction. For an *isolated molecule* of **1**, when the methyl group has rotated to the transition state, the methoxy group librates from its ground state angle of 40° (with respect to the adjacent benzene ring) to 57°. For an *isolated molecule* of **2**, when the methyl group has rotated to the transition state, the methoxy group librates from its ground state angle of 0° to 30°. For **1** *in the crystal*, when the methyl group has rotated to the transition state, the methoxy group librates from its ground state angle of 13° to 42°. For **2** *in the crystal*, when the methyl group has rotated to the transition state, the methoxy group librates from its ground state angle of 3° to 19°. The different angular methoxy group librations in **1** and **2** reflect predominantly the difference between there being H atoms or F atoms on the nearby ring. The differences between the isolated molecule and crystal values for the angular methoxy group libration angles corresponding to the methyl group transition state reflect the relative importance of intramolecular and intermolecular interactions.

(5) Considering only the *isolated molecules* of **1**, **2**, and **3**, the calculated methyl or fluoromethyl group barriers are 4.1 kJ mol^{-1} (methoxy group librating from 40° to 57°), 12.8 kJ mol^{-1}, (methoxy group librating from 0° to 30°) and 1.7 kJ mol^{-1} (involving a lone CF_3 group). The difference between the methyl group barriers in **1** and **2** might seem counterintuitive but barriers are *differences* between ground state energies and transition state energies and the presence of ring F atoms raises the energy of *both* states in **1** relative to those same states in **2**. The strong

methyl group H – ring F repulsion in **1** is present for all geometries. This is reflected in the fact that the methoxy group rotates only 17° in **1** (as the methyl group rotates over the barrier) whereas the methoxy group rotates 30° in **2**.

(6) The calculated methyl or fluoromethyl group barriers for a molecule in the center of a cluster of molecules based on the X-ray structure are 17.1 kJ mol^{-1} in **1** (methoxy group librating from 13° to 42°), 10.3 kJ mol^{-1} in **2** (methoxy group librating from 3° to 19°), and 10.9 kJ mol^{-1} in **3**. The methyl group barrier in the crystalline environment in **2** is *lower* than the barrier in the isolated molecule and the methoxy group libration angle is *reduced* from 30° to 16°. There are several competing interactions at work here but the result is that the ground state is raised in energy more than the transition state in going from the isolated molecule to the crystalline environment. The methyl group barrier in **1** is significantly higher than in the isolated molecule and the methoxy libration angle *increases* from 17° to 29°, just the opposite change from the change in **2**. Finally, the large increase in the fluoromethyl group barrier in **3** in going from the isolated molecule to the crystal results from the dominant contribution of the intermolecular interactions.

(7) The calculated methyl or fluoromethyl group barriers in the clusters compare favorably with the observed NMR activation energies E_{NMR} which are 16.5 ± 1.7 kJ mol^{-1} , 11.5 ± 0.5 kJ mol^{-1} , and 11.5 ± 0.7 kJ mol^{-1} in **1**, **2**, and **3**. This agreement provides support for both the NMR relaxation technique and the electronic structure calculation technique.

(8) The ^{1}H spin-lattice relaxation in **1** and **3** is nonexponential at low temperatures because the ^{1}H and ^{19}F spins interact via the unlike-spin dipolar interaction. The model that explains this phenomenon makes several distinct predictions. The biexponential relaxation of *both* spin species (^{1}H and ^{19}F) is characterized by the same two relaxation eigenrates of a 2 X 2 relaxation matrix. The various rates in this matrix can all be calculated from the Bloch-Wangsness-Redfield model. At low temperatures, both spin species relax with these same two rates (biexponential relaxation) whereas at high temperatures, where the relaxation is exponential, one of these eigenrates

corresponds to the rate for ^{1}H and the other to the rate for ^{19}F. The most interesting prediction of this model, in our opinion, is that the observed spin-lattice relaxation rates of the two spin species contain no constant multipliers involving the ratio of "mobile spins" (on the NMR time scale) to all spins (of the same spin species) in the molecule. This ratio is necessary in the theoretical expressions for the relaxation rate for single spin species relaxation.[1] This model introduces a parameter that characterizes the *ratio* of the strength of the methyl group ^{1}H – ring ^{19}F (or the fluoromethyl group ^{19}F – ring ^{1}H) dipolar interactions to that of the intramethyl group ^{1}H –^{1}H (or the intrafluoromethyl group ^{19}F –^{19}F) dipolar (spin-spin) interactions. This ratio is a *measure* of the difference of the two eigenvalue relaxation rates in the nonexponential relaxation process. This parameter[3] is $q = 0.020 \pm 0.005$ for **1** and $q = 0.055 \pm 0.010$ for **3**. If $q = 0$, the ^{1}H – ^{19}F interactions disappear and both the ^{1}H and ^{19}F relaxation is exponential and uncoupled at all temperatures.

(9) The ^{1}H spin-lattice relaxation in **1** and **2** is nonexponential at high temperatures because the motion of the three H–H vectors in a methyl group are 100% correlated and reorient in a plane. In compounds like **2**, where there are no ^{19}F spins, the relaxation rate that characterizes the initial recovery of the ^{1}H nuclear magnetization corresponds to the basic Bloch-Wangsness-Redfield model. In compounds like **2**, where there are both ^{19}F and ^{1}H spins (previous paragraph), the relaxation rate that characterizes the initial recovery of the ^{1}H nuclear magnetization is one of the eigenrates discussed in the previous paragraph.

(10) Thus, regardless of the complexities associated with the nonexponential relaxation, a rate or rates can be determined that corresponds to that given by, or easily derived from, the Bloch-Wangsness-Redfield theory of nuclear spin relaxation. An analysis of the parameters determined by fitting the NMR relaxation rates in the solid states of **1**, **2**, and **3**, show that the principle motion is the rotation, over a barrier, of CH_3 (or CF_3) groups. It is this motion, characterized by a mean frequency τ^{-1}, that is occurring on the NMR time scale. This parameter, $\tau = \tau_\infty \exp(E_{NMR}/kT)$, is the mean time

between CH_3 (or CF_3) hops in a random hopping process described by Poisson statistics. Perhaps the most useful parameter extracted from the relaxation rate data is the activation energy E_{NMR} that can be compared with the barrier calculated by electronic structure calculations. The parameter τ_∞ involves the moment of inertia of the rotating group with $\tau_\infty = \tilde{\tau}_\infty = (2\pi/3)(2I/E_{NMR})^{1/2}$ in the harmonic model.[39] This is indeed a crude model but the fitted values of $\tau_\infty / \tilde{\tau}_\infty = 0.3 \pm 0.2$ in **1**, $\tau_\infty / \tilde{\tau}_\infty = 0.8 \pm 0.2$ is in **2**, and $\tau_\infty / \tilde{\tau}_\infty = 0.4 \pm 0.1$ in **3** tell us, again, that the observed ^1H and/or ^{19}F spin lattice relaxation results from the modulation of the spin-spin dipolar interactions by methyl/fluoromethyl group rotation.

(11) The conceptual model for methyl or fluoromethyl group rotation is one where the group hops by 120° from one equilibrium position to an identical equilibrium position. The energy needed for such a hop is much greater than kT [e.g., 15 kJ mol^{-1} = k(1800 K)] so this hop happens when the group gets a kick from the thermal reservoir (phonons). In an NMR relaxation experiment, the average frequency of this random (Poisson) hopping process can be observed for approximately two orders of magnitude on either side of the NMR frequency of 22.5 MHz (which is the inverse of 4 x 10^{-8} s). On the NMR time scale, the time for a hop in this model is zero; it is instantaneous. The actual time for a hop is determined by the group vibrational time scale; say $\tilde{\tau}_¥ \approx 10^{-14}$ s in the simple harmonic model.[39]

(12) The positions of all H atoms in **1**, **2**, and **3** and the positions of the F atoms in the fluoromethyl group in **3** are determined by the electronic structure calculations in both the ground and transition states of the molecules in the clusters. The X-ray diffraction study in **3** showed the fluoromethyl group F atoms were disordered and this necessitated the positions being calculated. But for H atoms, the positions are difficult to measure accurately by X-ray crystallography. Using these calculated H positions is important in calculating the barriers for the various motions. But using the calculated H and F positions in methyl and fluoromethyl groups is *also* very important in interpreting the NMR relaxation rate.

(13) The fitted or calculated NMR relaxation parameters are consistent with the model that says CH_3 or CF_3 rotation (over a barrier) is responsible for the spin-lattice relaxation. However, the electronic structure calculations indicate that this CH_3 rotation is superimposed on methoxy group libration in **1** and **2**. The model for the NMR relaxation considers a random time-independent orientation of methyl group rotation axes[41] which is the case in a polycrystalline solid. The rapid methoxy group libration has no effect on the fitted NMR relaxation parameters and simply adds a rapid random time-dependence to the spatial randomness of the methyl group rotation axes in the polycrystalline sample. This is not to say that NMR relaxation experiments are not sensitive to superimposed motions. For example, these kinds of experiments can detect (and model) the superposition of methyl group and *t*-butyl group rotation.[42,43] But both these motions are on the NMR time scale. For **1** and **2**, the librational motion of the methoxy groups is much too fast to effectively modulate the spin-spin interactions. As such, a time average is indistinguishable (and only adds to) the spatial average due to the polycrystalline nature of the sample.

Acknowledgements

References

[1]Beckmann P. A.; Schneider E. *J. Chem. Phys.* **2012**, *136*, 054508, 1-9.

[2]Wang, X.; Rotkina, L.; Su, H.; Beckmann, P. A. *ChemPhysChem* **2012**, *13*, 2082-2089.

[3]Beckmann, P. A.; Rosenberg, J.; Nordstrom, K.; Mallory, C. W.; Mallory, F. B. *J. Phys. Chem. A* **2006**, *110*, 3947-3953. (Equation 1 should have a *d/dt* to the left of the left-hand side, as in equation 6 in this work.)

[4]Wang, X.; Mallory, F. B.; Mallory, C. W; Beckmann, P. A.; Rheingold, A. L.; Francl, M. M. *J. Phys. Chem. A*. **2006**, *110*, 3954-3960.

[5]Tilley R. *Crystals and Crystal Structures*; Wiley: Chichester, UK, 2006.

[6]Kimmich, R. *NMR Tomography, Diffusometry, Relaxometry*; Springer-Verlag: Berlin, 1997.

[7]Runnells L. K. *Phys. Rev.* **1964**, *134,* 28-36.

[8]Hilt, R. L.; Hubbard, P. S. *Phys. Rev.* **1964**, *134,* 392-398.

[9]Abragam, A. *The Principles of Nuclear Magnetism*; Oxford University Press: Oxford, UK, 1961.

[10]Bloch, F. *Phys. Rev.* **1956**, *102*, 104-135; Bloch, F. *Phys. Rev.* **1957**, *105*, 1206-1222.

[11]Redfield, A. G. *IBM J. Res. Develop.* **1957**, *1,* 19-31. Reprinted with minor revisions in *Advan. Mag. Reson.* **1965**, *1*, 1-32.

[12]Wangsness, R. K.; Bloch, F. *Phys. Rev.* **1953**, *89*, 728-739.

[13]Silverstein, R. M.; Webster, F. X. *Spectrometric Identification of Organic Compounds*; 6th ed. John Wiley and Sons: New York, 1998.

[14]Edholm O.; Blomberg, C. *Chem. Phys.* **1981**, *56*, 9-14.

[15]Kowalewski, J.; Liljefors, T. *Chem. Phys. Lett.* **1979**, *64*, 170-174.

[16]Clough, S. *Sol. State Nuc. Mag. Resonan.* **1997**, *9*, 49-53.

[17]Barlow, M. J.; Clough, S.; Horsewill, A. J.; Mohammed, M. A. *Sol. State Nuc. Mag. Resonan.* **1992**, *1*, 197-204.

[18]Clough, S., *Physica B* **1986**, *136*, 145-149.

[19]Cavagnat, D.; Clough, S.; Zelaya, F. O. *J. Phys. C: Sol. State Phys.* **1985**, *18*, 6457-6462.

[20]Clough, S.; McDonald, P. J.; Zelaya, F. O. *J. Phys. C: Sol. State Phys.* **1984**, *17*, 4413-4420.

[21]Clough S.; McDonald, P. J. *J. Phys. C: Sol. State Phys.* **1982**, *15*, L1039-L1042.

[22]Clough, S.; Heidemann, A.; Horsewill, A. J.; Lewis, J. D.; Paley, M. N. J. *J. Phys. C: Sol. State Phys.* **1981**, *14*, L525-L529.

[23]Clough, S.; Heidemann, A. *J. Phys. C: Sol. State Phys.* **1980**, *13,* 3585-3589.

[24]Stejskal, E. O.; Gutowsky, H. S. *J. Chem. Phys.* **1958**, *28*, 388-396.

[25]Diezemann, G. *App. Mag. Resonan.* **1999**, *17*, 345-366.

[26]Frisch, M. J.; Trucks, G. W.; Schlegel, H. B.; Scuseria, G. E.; Robb, M. A.; Cheeseman, J. R.; Montgomery, J. A., Jr.; Vreven, T.; Kudin, K. N.; Burant, J. C.; Millam, J. M.; Iyengar, S. S.; Tomasi, J.; Barone, V.; Mennucci, B.; Cossi, M.; Scalmani, G.; Rega, N.; Petersson, G. A.; Nakatsuji, H.; Hada, M.; Ehara, M.; Toyota, K.; Fukuda, R.; Hasegawa, J.; Ishida, M.; Nakajima, T.; Honda, Y.; Kitao, O.; Nakai, H.; Klene, M.; Li, X.; Knox, J. E.; Hratchian, H. P.; Cross, J. B.; Bakken, V.; Adamo, C.; Jaramillo, J.; Gomperts, R.; Stratmann, R. E.; Yazyev, O.;

Austin, A. J.; Cammi, R.; Pomelli, C.; Ochterski, J. W.; Ayala, P. Y.; Morokuma, K.; Voth, G. A.; Salvador, P.; Dannenberg, J. J.; Zakrzewski, V. G.; Dapprich, S.; Daniels, A. D.; Strain, M. C.; Farkas, O.; Malick, D. K.; Rabuck, A. D.; Raghavachari, K.; Foresman, J. B.; Ortiz, J. V.; Cui, Q.; Baboul, A. G.; Clifford, S.; Cioslowski, J.; Stefanov, B. B.; Liu, G.; Liashenko, A.; Piskorz, P.; Komaromi, I.; Martin, R. L.; Fox, D. J.; Keith, T.; Al-Laham, M. A.; Peng, C. Y.; Nanayakkara, A.; Challacombe, M.; Gill, P. M. W.; Johnson, B.; Chen, W.; Wong, M. W.; Gonzalez, C.; Pople, J. A. *Gaussian 03*, revision B.05; Gaussian, Inc.: Wallingford, CT, 2004.

[27]Stephens, P. J.; Devlin, F. J.; Chabalowski, C. F.; Frisch, M. J. *J. Phys. Chem.* **1994**, *98*, 11623-11627.

[28]Becke, A. D. *J. Chem. Phys.* **1993**, *98*, 5648-5652.

[29]Lee, C.; Yang, W.; Parr, R. G. *Phys. Rev. B* **1988**, *37*, 785-789.

[30]Vosko, S. H.; Wilk, L.; Nusair, M. *Can. J. Phys.* **1980**, *58*, 1200-1211.

[31]McLean, A. D.; Chandler, G. S. *J. Chem. Phys.* **1980**, *72*, 5639-5648.

[32] Raghavachari, K.; Binkley, J. S.; Seeger, R.; Pople, J. A. *J. Chem. Phys.* **1980**, *72*, 650-654.

[33] Wang, X.; Beckmann, P.A.; Mallory, C. W.; Rheingold, A. L.; DiPasquale, A. G.; Carroll, P.; Mallory, F. B. *J. Org. Chem.* **2011**, *76*, 5170-5176.

[34]Deringer, V. L.; Hoepfner, V.; Dronskowski, R. *Cryst. Growth Des.* **2012**, *12*, 1014–1021.

[35]Steiner, T; Saenger, W. *Acta Cryst.* **1993**, *A49*, 379-384.

[36]Wang, X.; Rheingold, A. L.; DiPasquale, A. G.; Mallory, F. B.; Mallory, C. W.; Beckmann, P. A. *J. Chem. Phys.* **2008**, *128*, 124502, 1-3.

[37]Slichter C. P. *Principles of Magnetic Resonance*, 3rd ed; Springer-Verlag: Berlin, 1990.

[38]Ernst, R. R.; Bodenhausen, G.; Wokaum, A. *Principles of Nuclear Magnetic Resonance in One and Two Dimensions*; Oxford University Press: Oxford UK, 1987.

[39]Owen, N. L. in *Internal Rotation in Molecules*; edited by W. J. Orville-Thomas, Wiley: New York, 1974.

[40]Rajeswari, M.; Molugu, T. R.; Dhara, S.; Venu, K.; Sastry, V. S. S.; Dabrowski, R. *Chem. Phys. Lett.*, **2012**, *531*, 80-85.

[41]Palmer, C. A.; Albano, A. M.; Beckmann, P. A. *Physica B* **1993**, *190*, 267-284.

[42]Popa, L. C.; Rheingold, A. L.; Beckmann, P. A. *Sol. State Nuc. Mag. Resonan.* **2010**, *38*, 31-35.

[43]Beckmann, P. A.; Dougherty Jr., W. G.; Kassel, W. S. *Sol. State Nuc. Mag. Resonan.* **2009**, *36*, 86-91.

Table 1. Comparison of parameters for the calculated isolated molecule structure and the X-ray crystallographic structure of the 4,4'-dimethoxyoctafluorophenyl molecule

Parameters[a,b]	X-ray (100 K)	X-ray (200 K)	Calc
Bond Lengths (Å)			
C1-C1^l	1.482(3)	1.484(4)	1.481
C1-C2	1.397(2)	1.393(3)	1.396
C2-C3	1.377(2)	1.374(3)	1.385
C3-C4	1.400(2)	1.392(3)	1.402
C4-C5	1.395(2)	1.394(3)	1.399
C5-C6	1.382(2)	1.380(3)	1.388
C6-C1	1.385(2)	1.382(3)	1.393
C2-F	1.340(2)	1.336(2)	1.341
C3-F	1.341(2)	1.339(2)	1.338
C5-F	1.346(2)	1.341(2)	1.347
C6-F	1.343(2)	1.341(2)	1.341
C4-O	1.348(2)	1.350(3)	1.347
O-Cm	1.445(2)	1.435(3)	1.441
RMSD	0.003^c		0.004^d
Bond Angles (º)			
C2-C1-C1^l	122.6(2)	122.7(2)	121.8
O-C4-C5	127.7(2)	128.2(2)	125.7
Cm-O-C4	120.5(2)	120.0(1)	119.6
Bond Dihedral Angles (º)			
C2-C1-C1^l-C6^l	−58.0(2)	−57.4(1)	−62.5
Cm-O-C4-C5	13.4(4)	13.0(2)	40.0

^{a}Since the two 4-methoxytetrafluorophenyl groups are equivalent in both the calculated (isolated molecule) and experimental structures, only the parameters of one part or between the two parts are given.
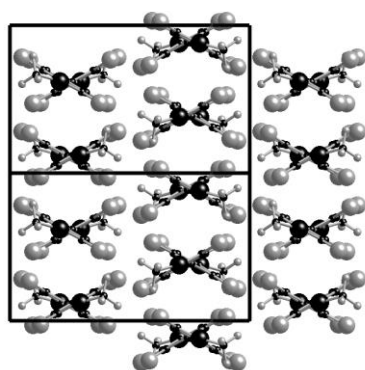
^{b}Atom labeling is indicated in Figure 1.

^{c}Root mean square deviation between the 100 K and the 200 K X-ray values in the crystal.

^{d}Root mean square deviation between the calculated values in the isolated molecule and the average of the 100 K and 200 K X-ray values in the crystal.
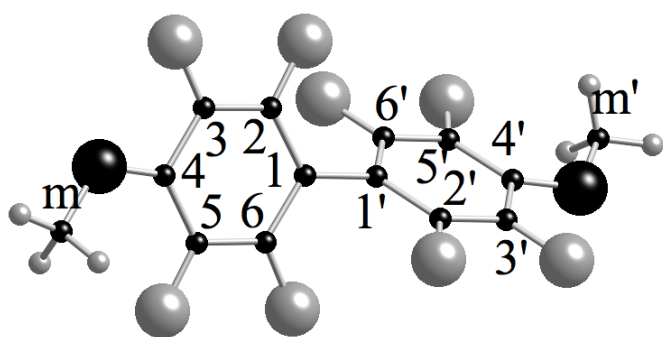
(a)

(b)

Figure 1. The molecular and crystal structure of 4,4'-dimethoxyoctafluorobiphenyl (**1**). The large black spheres are oxygen atoms, the large grey spheres are fluorine atoms, the small black spheres are carbon atoms, and the small grey spheres are hydrogen atoms, all of which are in methyl groups. **(a)** The structure of the molecule, which, at the scale shown, is the same for the isolated molecule as determined by electronic structure calculations as it is in the crystal as determined by x-ray diffraction. The view is such that all atoms are visible. The carbon atoms are labeled. **(b)** A view of the crystal structure in the 100 plane. Unit cells are shown. The horizontal axes are the *z*-axes and the vertical axes are the *y*-axes. The 19 molecules shown (some behind others) correspond to the cluster used in the electronic structure calculations. **(c)** The same 19 molecules corresponding to the cluster shown in (b). This view is rotated by 3° about the *z*-axes away from the 010 plane and all 19 molecules in the cluster can be seen. Unit cells are shown. The horizontal axes are the *x*-axes and the vertical axes are the *z*-axes.
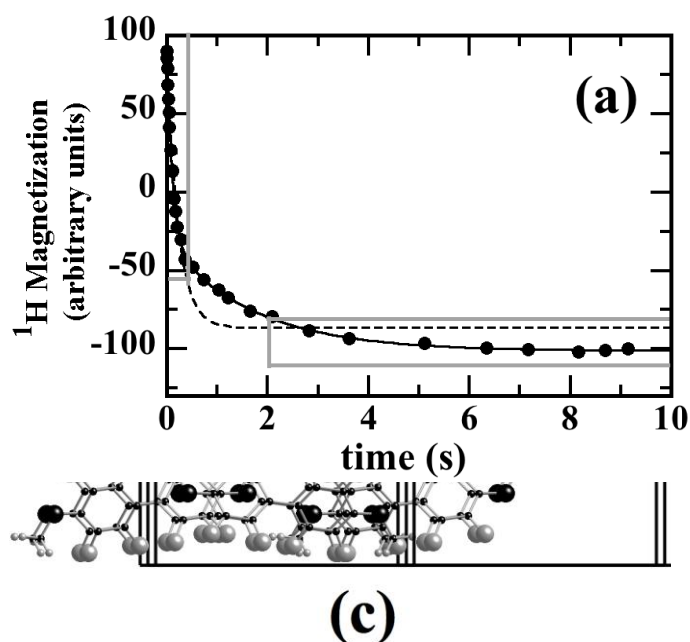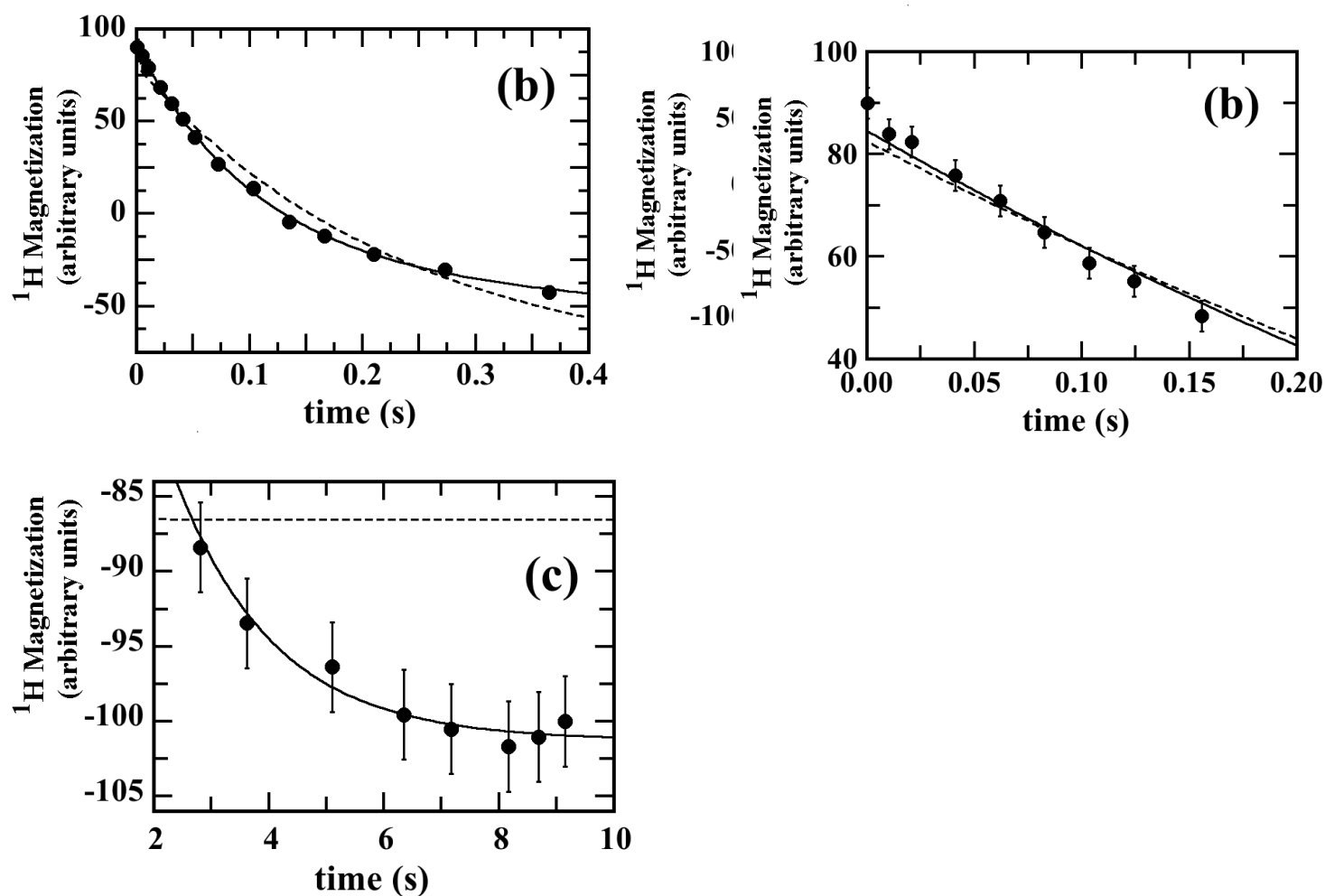
Figure 2. The ^{1}H magnetization recovery in an inversion recovery experiment at $1000/T = 8.76$ K^{-1} ($T = 114$ K) in polycrystalline 4,4'-dimethoxyoctafluorobiphenyl (**1**). This is in the low temperature regime III indicated in Figure 4. The solid line is a double exponential fit (giving λ_1 and λ_2) and, for comparison, the short-dashes line is a single exponential fit. **(a)** The entire recovery curve. **(b)** The short-time recovery indicated by the grey box at the upper-left-hand corner of part (a). **(c)** The long-time recovery indicated by the grey box at the lower-right-hand corner of part (a). The uncertainties are shown but are within the size of the symbols in (a) and (b).
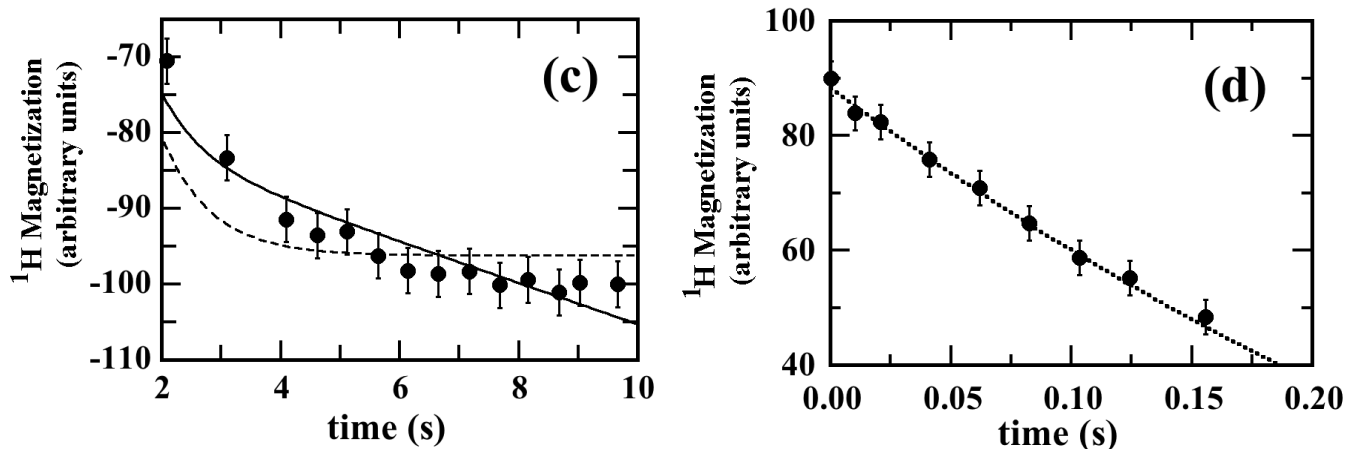
Figure 3. The ^{1}H magnetization recovery in an inversion recovery experiment at $10^3 \, T^{-1} = 4.00$ K^{-1} ($T = 250$ K) in polycrystalline 4,4'-dimethoxyoctafluorobiphenyl (**1**). This is in the high-temperature regime I indicated in Figure 4. **(a)** The entire recovery curve. **(b)** and **(d)** The short-time recovery indicated by the very small grey box at the upper-left-hand corner of part (a). **(c)** The long-time recovery indicated by the grey box at the lower-right-hand corner of part (a). **(a), (b), and (c)** Using all 10 s of data, the solid line is a double exponential fit and the short-dashes line is a single exponential fit. Neither are successful. **(d)** The heavy dotted line uses only the first 0.17 s of data, namely that which is shown, to fit to a single exponential.
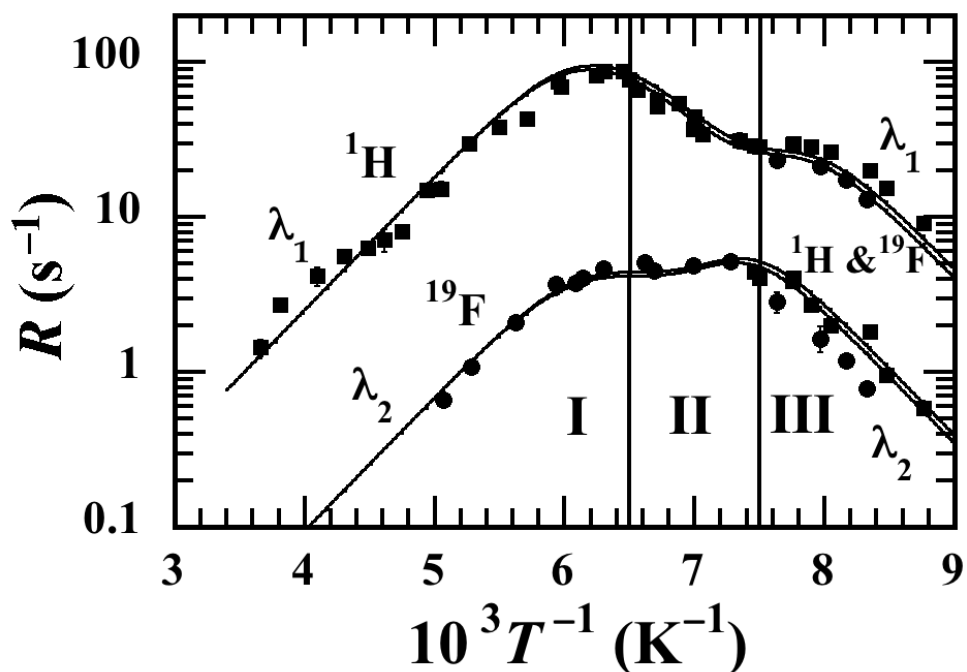
Figure 4. ^{1}H (□) and ^{19}F (□) $\ln\lambda_1$ and $\ln\lambda_2$ versus T^{-1} in polycrystalline 4,4'-dimethoxyoctafluorobiphenyl (**1**) *both* at an NMR frequency of 22.5 MHz.   The vertical lines at $10^3\,T^{-1} = 6.5$ and 7.5 K^{-1} separate the three temperature regions I, II, and III.
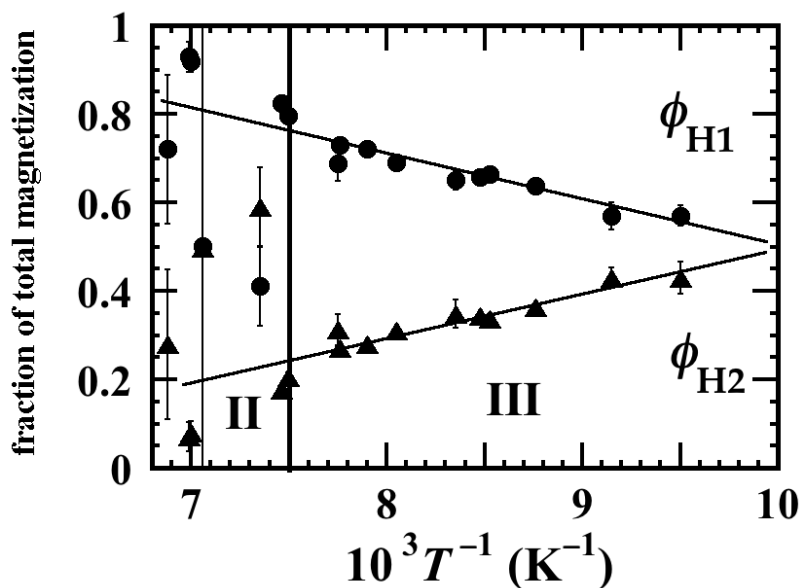
Figure 5. The fractions ϕ_{H1} (□) and ϕ_{H2} (□) of the ^{1}H magnetization associated with the rates λ_1 and λ_2 respectively in a double exponential fit of the relaxation versus T^{-1} in polycrystalline 4,4'-dimethoxyoctafluorobiphenyl (**1**) at an NMR frequency of 22.5 MHz in the low temperature region III and part of the middle temperature region II. The vertical line at $10^3 T^{-1} = 7.5$ K^{-1} separates the two temperature regions. The vertical line at $10^3 T^{-1} = 7.05$ K^{-1} is actually an uncertainty bar. The predicted linear dependence of the two magnetizations ϕ_{H1} and ϕ_{H2} characterizing the double exponential relaxation in the low temperature region III is shown by the solid lines. The two lines sum to 1. The double-exponential fit is not successful in region II.